Shear Flow and Mixing of Cohesive and Lubricated Granular Material

A Thesis

submitted to

Indian Institute of Science Education and Research Pune

in partial fulfillment of the requirements for the

BS-MS Dual Degree Programme

by

Chinmay Katke

Indian Institute of Science Education and Research Pune

Dr. Homi Bhabha Road,

Pashan, Pune 411008, INDIA.

April, 2019

Supervisor: Dr. Ashish Orpe

© Chinmay Katke 2019

Certificate

This is to certify that this dissertation entitled Shear Flow and Mixing of Cohesive and Lubricated Granular Material towards the partial fulfilment of the BS-MS dual degree programme at the Indian Institute of Science Education and Research, Pune represents study/work carried out by Chinmay Katke at Indian Institute of Science Education and Research under the supervision of Dr. Ashish Orpe , Scientist, Chemical Engineering and Process Development Division, CSIR-National Chemical Laboratory, Pune , during the academic year 2018-2019.

Dr. Ashish Orpe

Committee:

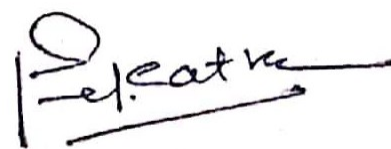Dr. Ashish Orpe

Prof. Deepak Dhar

To my ever supportive parents and my friends at IISER

Declaration

I hereby declare that the matter embodied in the report entitled Shear Flow and Mixing of Cohesive and Lubricated Granular Material are the results of the work carried out by me at the Chemical Engineering and Process Development Division, CSIR-National Chemical Laboratory, Pune, Indian Institute of Science Education and Research, Pune, under the supervision of Dr. Ashish Orpe and the same has not been submitted elsewhere for any other degree.

Chinmay Katke

Acknowledgments

x

Abstract

The grains of the pharmaceutical powder have frictional and cohesive interaction between them. This creates problems during tablet ejection, reduces the flow properties and increases the losses due to particle sticking to the surface. To overcome this difficulties small concentration of powder lubricant is added to the blend. The lubricant powder sticks to the surface of the grain to reduce the friction and cohesion and thereby improving the flow properties. The Objective of this work is to analyze the coating of the lubricant particle around the drug particles and to understand the role of the lubricant in the improving the flow properties using DEM simulations of spherical particles. The DEM simulations are carried out using open source LIGGGHTS software, which allows for the independent choices of particle size, cohesion strength and coefficient of friction. The blend particles and lubricant particles were modeled as large sized, rough ($\mu = 0.5$),spherical and small sized, spherical with lesser frictional interaction ($\mu = 0.05$) respectively. We studied two mechanism of lubrication viz, lubrication by reducing friction between large particles and lubrication by reducing cohesion between large particles in the parallel plate shear geometry in the presence as well as absence of gravitational field for the range of lubricant concentration and lubricant size. The modified shear behavior was quantified in terms of granular flux for the constant applied torque to the system. In the latter mechanism of lubrication, for a range of particle number ratio and size ratio studied, the flux shows an increase with increase in number ratio and decrease in size ratio. Both variation seem to increase the number of lubricant particles between large particles, thereby preventing the contact which results in less cohesive interaction in the flow as a result flow behavior gets modified.

Contents

List of Figures

1

List of Tables

Introduction

Granular matter is everywhere around us, from natural occurrences like sand dunes to consumer products like talcum powder. Though it is present in abundance, we do not understand granular matter very well. Granular matter comprises of particles with size ranging from few microns to few centimeters [1]. The interaction between these particles are dissipative nature and may involve various forces like friction and cohesion. Granular matter exhibit properties of both solid and liquid. While sand flows in hour glass under the action of gravitational force like liquid, heap of sand supports the weight of itself like a solid.

Granular materials are encountered in several industrial processes, one of them being tablet manufacturing in pharmaceutical industry. A tablet is a mixture of several ingredients comprising active drugs and excipient particles [2]. Most of these ingredients are in powder form. The grains of these powders have inherent friction between them and also with walls of the tablet press which causes wear and during in tablet compression and ejection.

To overcome these problems, a very small concentration of powder lubricant is added to the blend, most common being Magnesium Stearate [3]. These lubricant particles are plate like in shape and are characterized by small size, high surface to volume ratio, low inter particle friction, hydrophobic nature and low shear strength. While the optimality of lubricant concentration with respect to performance is reasonably understood, the detailed mechanism is not clear[4]. There are two possible ways to lubricate the mixture. First one is by reducing the friction between two large particles which is the tangential force between two particles acting in direction opposite to the motion of the particle and second one by reducing the cohesive force between the two which is the attractive force between two particles acting in normal direction. Higher friction and cohesion have adverse effect on flow properties of the powder. The presence of the lubricant particles facilitates easier tablet ejection, improved flowability, improved product uniformity and overall product quality [3, 5]. Investigating

the possible mechanisms of lubrication, their correlation with the dynamics and distribution of surface coating and the overall effect of lubrication on powder flowability is the primary objective of this work.

The work incorporates Discrete Element Method (DEM) simulations methodology with both powder and lubricant particles modeled as spherical grains sheared in parallel a plate geometry. There are few limitation in mimicking the plate like lubricant particles with spherical ones. The plate like particles primarily have sliding friction between them due to higher surface area and spherical particles have rolling friction between them. Also plate like particles have higher surface area to volume ratio than the spherical particles. Hence to coat the large particles effectively like plate particles, the size of the spherical lubricant particles was reduced and number was increased consequently to maintain near constant volume. Reduced size increased the surface area to volume ratio of the lubricant particles and increased number allowed larger coverage of surface area of rough particle.

The thesis is organized as follows. Chapter one reviews the simulations and experiments on granular flows relevant to this work. The significant studies of the pharmaceutical lubrication are also summarized in this chapter. Chapter two provides the details of the Discrete Element Method(DEM) and simulation setup used in this work. Chapter three and four provide the details about simulations done to explore friction reduction nature of the lubricant and cohesion reduction nature of lubricant. The conclusions are provided in chapter five.

Chapter 1

Literature Review

Granular flow properties can be categorized into three classes. The first class is characterized by low inertia which can be described by soil plasticity model[6]. The second one is characterized by high inertia where grains collide with each other frequently and are in less contact which each other, thus lesser friction. This phase can be modelled using kinetic theory[7, 8]. The third one is called dense granular flows and is dominated equally by friction and collision between particles. Though grains have higher velocities, they still have enduring contacts[9]. We are interested in this third type of flows. In this chapter we provide a brief review about dense granular flows followed by describing relevant literature to powder lubrication.

1.1 Granular Flow Systems

Various types of dense granular flows were reviewed by French research group Groupement De Recherche Milieux Divises (GDR MiDi) [10]. The review provides several experimental as well simulation studies in various geometries. Dense Granular flows are typically studied in six primary geometries(fig 2.1). In parallel plate shear, grains are confined within two parallel plate and one plate is moved in direction parallel to plane to shear the system(fig 1.1a). This is the special case of annular shear for both radii are tending to infinity [11]. The velocity profile for parallel plate shear is exponential [11]. In annular shear flow, grains are sheared in between two concentric cylinder by rotating one of them (fig 1.1b). The shear is localized within 5 to 6 particle diameter from the moving wall and particles further

away from the wall are practically immobile [12]. The velocity profile in shear zone is of exponential nature. In vertical silo flow grains are allowed to flow between two parallel walls under the action of gravity (fig 1.1c). The velocity profile is characterized by plug flow in central region and variation in two small regions near the wall [13]. The flow on the rough inclined plane is show in fig 1.1d. Velocity profile is nonlinear with polynomial function of flow height [14]. In the heap flow and rotating drum, flows are confined to the surface of the static granular bed. Both flows are comprised of upper linear part in flowing layers and exponential part in granular bed [15, 16]. While parallel plate shear, annular shear and vertical chute flow are the confined flows; inclined plane, heap flow and rotating drum are free surface flows. Apart from parallel plate shear and annular shear other flows are gravity driven.
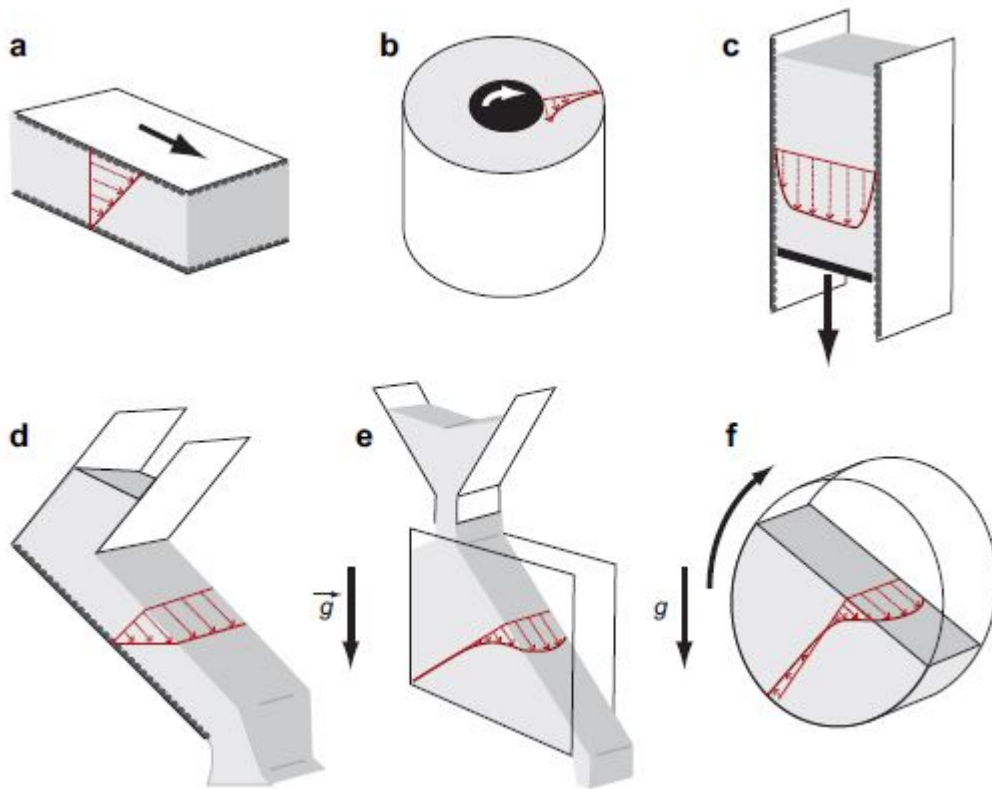
Figure 1.1: a)Parallel plate shear b)Annular shear c)Vertical chute flow d)Inclined plane e)Heap flow f)Rotating drum

1.2 Granular matter as a lubricant

The lubricant properties of granular matter are reviewed in this section. First we review the use of granular matter as a replacement for traditional liquid lubricants in mechanical systems and in latter part use of lubricant powders to lubricate granular flows are discussed.

1.2.1 Tribology

The use of liquid lubricants such as grease and engine oil between sliding surfaces is quite well known. In recent years, powders have been explored as replacement of lubricants [17]. These lubricants serve as replacement for traditional lubricants in extreme environments like extreme temperature and loads[18]. The presence of powder between two shearing substrates results in two co-existing zones, viz., interface between powder and the substrate, and the bulk powder region accompanied by the powder undergoing different modes of behavior, viz., elastic deformation, plastic deformation, shearing and rolling [19, 20]. A detailed experimental study of the underlying details of the above lubrication process was carried out by Berthier [21] thereby providing a firm basis for theoretical modeling which was later on extended by Descartes et al. to study in detail the contact dynamics between substrate and lubricant powder leading towards the friction coefficient[22]. The concepts mentioned above were used in discrete simulation to obtain fundamental mass balance laws by Fillot [23] and by Iordanoff to obtain the effect of powder characteristics on the overall frictional [24]. Though use of powders and grains as a replacement to traditional lubricants is well studied, it may not easily translated to the case of powder (small particles) lubricating the granular flows comprising larger particles. The studies focused on this aspect of the lubrication are reviewed next. properties.

1.2.2 Lubrication in Pharmaceutical Powders

Pharmaceutical industry largely deals with dense granular flows. To increase the efficiency of these flows often lubricants are used. Lubrication in pharmaceutical powders is different than the tribology. While in tribological terms granular matter is used to reduce the friction between two mechanical surfaces, in pharmaceutical industries, the lubricant powder is used

to improvise the flow properties another bulk powder flow.[4].

Muzzio et al. studied the flow properties of the mixture of carrier particles, API particles and magnesium stearate in advanced couette flow geometry comprised of baffles in the shearing zone to impart nearly uniform shear [25]. They observed increased bulk density, reduced cohesion, reduced angle of internal friction, and reduced compressibility. It was also observed that extent of lubrication is highly dependant on shear time rather than shear energy. This decides under-lubrication, optimal lubrication and over-lubrication of the blend. Both under-lubrication and over-lubrication are highly undesired as under lubrication leads to wearing and particle losses while over lubrication leads to decreased tablet tensile strength. Mechanism of the lubrication is attributed to reduction in frictional and/or cohesion forces between two grains [26, 27]. Cohesive force between two grains depend upon the interparticle distance [28]. Presence of lubricant particles causes increase in the inter-particle distance between two particle which leads to decrease in cohesive force [29]. Lubricant particles also coat the surface of the rough blend particles to improve the frictional properties [3]. Similar behavior was observed in other shear geometries like rotating drum , vibrated systems[25], and feed frame flows [30]

Very less is known about the distribution of the lubricant particles around the rough particles. Since lubricant is in very low concentration it is very hard to detect it in the mixture. Energy-dispersive X-ray microanalysis was used by Hodi et al to detect the variable lubricant film thickness [31]. Lubricant layer was found out to be patchy than continuous [32]. Raman Spectroscopy method was used by Lakio et al to map the concentration of Magnesium Stearate on the surface of the tablet [3]. This process only maps the surface of the tablet and no information is gained about the distribution of lubricant inside the bulk. The process is also time consuming and demands precision.

Tablet manufacturing involves compression of tablet blend to form tablet which causes rearrangement of blend particles [33]. They mechanical strength of tablet was found out to be decreasing with increasing degree of mixing of the lubricant [34]. Scale up models for tensile strength of tablet has been proposed [35]. The tensile strength of tablet and ingredient distribution inside tablet represent the another facet of powder lubrication.

All the works discussed above are very specific to particular blend and particular lubricant used to lubricate that blend. There is very little understanding about the mechanism of lubrication. The generalized understanding of this mechanism based only upon the prop-

erties of particles like size, cohesion strength and concentration of the lubricant can give many useful insights. Obtaining insights based on such parameters would help to reduce the wastage of drug in the tablet manufacturing. The objective of this work is to analyze the coating of the lubricant particle around the drug particles and to understand the mechanism of lubrication in the improving the flow properties using DEM simulations of spherical particles. The dependence of lubrication on the lubricant parameters like concentration and lubricant size will also be examined along with the spatial distribution of lubricant particles over the surface of the rough particle and also in the bulk of the mixture.

For this work, we chose parallel plate shear to study granular lubrication which is the simplest of all to implement in DEM simulations [10]. Parallel plate geometry provides us shear driven flow. The parallel plate geometry allows for studying the flows in presence or absence of gravity which is not possible in systems where flows are gravity driven. Though all the real life systems have gravity embedded in it, gravity less flow provides uniform shear through out the system necessary for uniform mixing of the lubricant. Absence of gravity prevents segregation of lubricant particles, reduces flow localization and observe the effect of pure shear. Achieving uniformity in presence of gravity involves complex geometry which was not possible to construct in open-sourced version of LIGGGHTS [36]. Furthermore it provides control over shear in the system by moving the wall with constant velocity or by applying constant torque on the wall. Finally, the verification of the results is easily possible by carrying out experiments in an annular shear geometry.

Chapter 2

Methodology

The detailed description of the overall methodology is presented in this chapter. A brief overview about Discrete Element Method (DEM) is provided first followed by information about the LIGGGHTS, the open source DEM simulator used for all the simulations in this work. The last section provides information about various systems incorporated in the work.

2.1   Brief review of the DEM simulations

DEM simulations were developed by Cundall and Stark [37]. It is very similar to molecular dynamics simulations with interactive forces between a pair of a particles described by Hertzian contact force model. Details of this contact model are described in later section of this chapter. DEM simulations are effectively used to model the granular and discontinuous material like granular flows, powder mechanics and rock mechanics. Below are the key steps in the DEM simulation techniques.

• **Initialization :** Initializing the co-ordinates of the position and velocities of the each atom or the grain.

• **Ensemble and Interaction :** Building of the list of neighbors for every particle present inside force cut off distance and then calculating the total force on the each particle. Force cut off distance is a radius of the hypothetical sphere centered at center of the parti-

cle. Typically, all the particles present inside the force cut-off distance are considered as a neighbor. Interaction with each of the neighbor is added to calculate the total force on the particle. Mainly three types of ensembles are used in molecular dynamics

i) **NVE** - Where number of atoms, volume and energy are kept constant. This is called Micro-cannonocal ensemble.

ii) **NPT** - Where number of atoms, pressure and temperature are kept constant.

iii) **NVT** - Where number of atoms, volume and temperature are kept constant.

Statistically, instantaneous temperature can be found by equating $\frac{1}{2}nK_bT$ to average kinetic energy. Keeping temperature constant results in constant kinetic energy which is not valid for granular matter due to dissipative interactions. Hence we chose NVE ensemble for the integration [38]

• **Integration :** The particles in the DEM simulations follow the Newton's law of the motion [37]

$$f = ma = m\frac{dv}{dt} = m\frac{d^2r}{dt^2} \tag{2.1}$$

Acceleration of the each particle is calculated by dividing the total force on the particle by its mass.

To integrate the position of the particles, the Velocity-Verlet algorithm is used [39]. Basic Verlet algorithm involves Taylor expansion of the position the particle as function of the time.

$$r(t + \delta t) = r(t) + v(t)\delta t + \frac{1}{2}a(t)\delta t^2 + \frac{1}{6}b(t)\delta t^3 + O(t^4) \tag{2.2}$$

$$r(t - \delta t) = r(t) - v(t)\delta t + \frac{1}{2}a(t)\delta t^2 - \frac{1}{6}b(t)\delta t^3 + O(t^4) \tag{2.3}$$

Adding both equation and ignoring the fourth order terms for very small δt gives us

$$r(t + \delta t) = 2r(t) - r(t - \delta t) + a(t)\delta t^2 \tag{2.4}$$

Here we identify a(t) as the acceleration of the particle. Using this relation, co-ordinates of the particle can be calculated for subsequent timestep except for first timestep. For the first timestep, $r(t - \delta t)$ is not defined. This is fixed by Velocity-Verlet algorithm which incorporates position and velocity at the same timestep [40].

$$r(t + \delta t) = r(t) + v(t)\delta t + \frac{1}{2}a(t)\delta t^2 \tag{2.6}$$

16
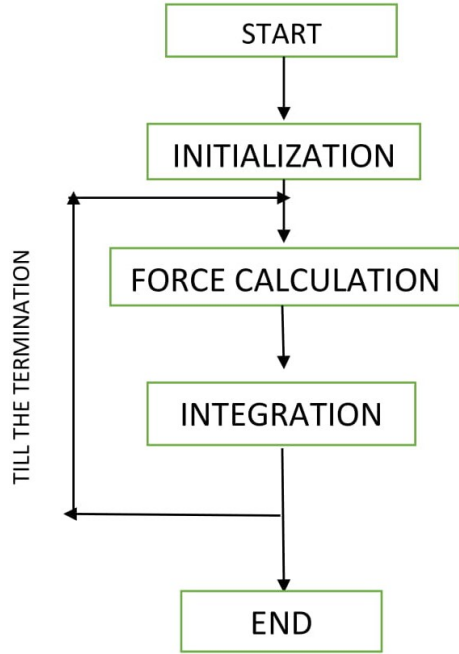
Figure 2.1: Flow Chart describing DEM simulation

$$v(t + \delta t) = v(t) + \frac{a(t) + a(t + \delta t)}{2} \delta t \tag{2.7}$$

using equation 2.6 and 2.7 the positions of the each of the particles are updated at each timestep.

•**Analysis :** Various quantities like stress, kinetic energy, potential energy etc. are computed using values from simulation output. Steps 2 to 4 are repeated until the termination of the simulation. The schematic of flow chart is shown below in fig.2.1.

2.2 Simulation Program (LIGGGHTS)

LIGGGHTS is a open source DEM simulator. LIGGGHTS stands for **L**AMMPS **I**mproved for **G**eneral **G**ranuar and **G**ranular **H**eat **T**ransfer **S**imulation. LAMMPS is molecular dy-

17

namics simulator developed by Sandia National Laboratry, US Department of Energy. It stands for **L**arge-scale **A**tomic/**M**olecular **M**assively **P**arallel **S**imulator [41, 42]. LIGGGHTS is developed by Christoph Kloss of Christian Doppler Laboratory, Johannes Kepler University, Austria [43, 44]. Below we discuss the two types of forces between two grains, namely Hertzian contact force and cohesive force as implemented by the LIGGGHTS.

2.2.1 Hertzian Contact Model

Grains are modelled as a soft, frictional and spherical particles. Though these particles are deformable, a large amount of force is required to deform them. When distance between two spherical particles is greater than the sum of their radii, r_i and r_j respectively, there is no force between them (see fig. 2.2). When the distance is less than the sum of their radii, there is finite overlap between two particles. This results in repulsive force which is modeled by following equation 2.7 [45]

Grains approaching   Overlap in contact   Repulsion after collision
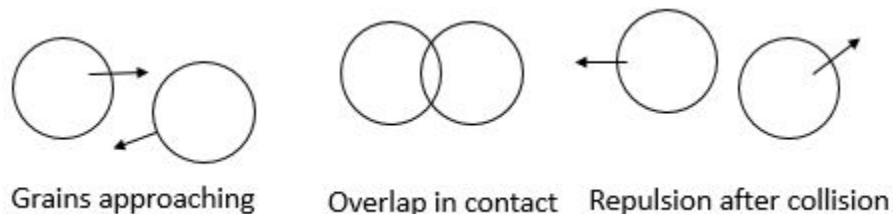
Figure 2.2: The Hertizian contact force is a finite repulsive force between two grains during the collision. The figure shows three stages of collision.

$$F = (k_n \delta n - \gamma_n v_n) + (k_t \delta t - \gamma_t v_t) \tag{2.7}$$

F - total force
k_n - elastic constant of normal overlap
δn - normal overlap between two particles
γ_n - viscoelastic damping constant for normal contact
v_n - normal component of relative velocity of two grains
k_t - elastic constant for tangential overlap
δt - tangential overlap between two particles

γ_t - viscoelastic damping constant for tangential contact

v_t - tangential component of the relative velocity

The quantity in the first bracket gives the normal component of total force while quantity in second bracket gives tangential component of total force acting on each particle. Values of the tangential force is truncated so that Coulomb's criterion for the friction is satisfied.

$$F_t \leq \mu F_n \tag{2.8}$$

Values of elastic and damping constants are calculated using the material properties like Young's Modulus (Y_i), Poisson's Ratio(ν_i), and coeff. of restitution (e_{ij}) [45].

$$k_n = \frac{4}{3} Y^* \sqrt{R^* \delta n} \tag{2.9}$$

$$\gamma_n = -2\sqrt{\frac{5}{6}} \beta \sqrt{S_n m^*} \geq 0 \tag{2.9}$$

$$k_t = 8 G^* \sqrt{R^* \delta n} \tag{2.10}$$

$$\gamma_t = -2\sqrt{\frac{5}{6}} \beta \sqrt{S_t m^*} \geq 0 \tag{2.11}$$

$$S_n = 2 Y^* \sqrt{R^* \delta n} \tag{2.12}$$

$$S_t = 8 G^* \sqrt{R^* \delta n} \tag{2.13}$$

$$\beta_{ij} = \frac{\ln e_{ij}}{\sqrt{(\ln e_{ij})^2 + \pi^2}} \tag{2.14}$$

$$\frac{1}{Y^*} = \frac{(1 - \nu_i^2)}{Y_i} + \frac{(1 - \nu_j^2)}{Y_j} \tag{2.15}$$

$$\frac{1}{G^*} = \frac{2(2 - \nu_i)(1 + \nu_i)}{Y_i} + \frac{2(2 - \nu_j)(1 + \nu_j)}{Y_j} \tag{2.16}$$

$$\frac{1}{R^*} = \frac{1}{R_i} + \frac{1}{R_j} \tag{2.17}$$

$$\frac{1}{m^*} = \frac{1}{m_i} + \frac{1}{m_j} \tag{2.18}$$
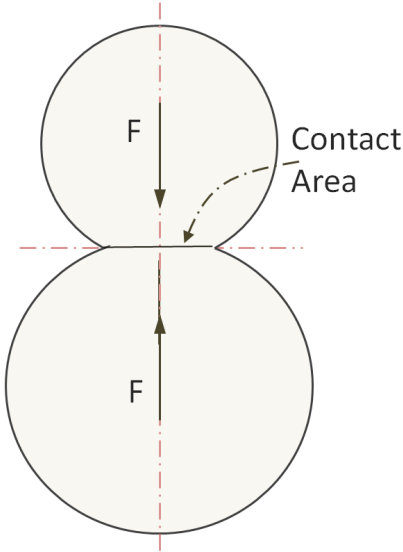
Figure 2.3: **Cohesive Force**. The cohesive force between two grains is directly proportional to the contact area between two grains and acts radially inward towards center

2.2.2 Cohesive Force

The cohesive force is modeled using Johnson-Kendall-Roberts (JKR) model [46]. This adds the attractive force on the grains in contact with each other. This force is directly proportional to the contact area between the two touching grains (A) [47]. The cohesive force is only present when two grains are in contact.

$$F_{coh} = kA \tag{2.19}$$

where constant of proportionality k is called cohesion energy density.

2.3 System Details

2.3.1 Geometry

Different types granular flow systems were discussed in the previous chapter. We chose the parallel plate geometry to study the shear flow properties of the mixture (see fig. 2.4). It is the special case of the widely used annular shear flow in the limit of both inner and outer

radius tending to infinity. The shear cell is periodic in flow (x) direction. Periodic boundary condition implies particle moving from one boundary enters in the shear cell from opposite boundary. Also particles from one boundary interact with the particles from opposite boundary. This simplification greatly reduces the number of atoms in the simulation and mimics a continuous system away from boundaries.
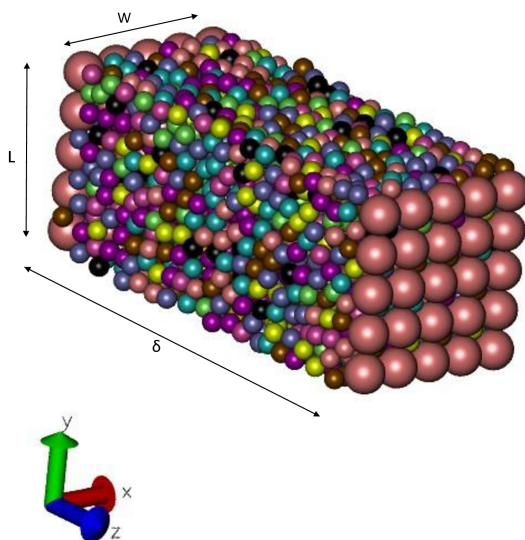
Figure 2.4: Schematic of a parallel plate geometry. The flow occurs in x-direction while being sheared in z-direction by walls separated by distance δ. The y-direction represents the neutral direction.

As shown in the fig. 2.4, The particles are sheared in a rectangular box, by moving the z-walls with constant velocity or by applying constant torque in x-direction. Different types of walls and several box dimensions were studied and the details of which are mentioned in the next chapter at appropriate locations. Different protocols used for setting up the system and studying shear therein are briefly described below. This primarily cover the parametric space explored in this work

21

In the presence of the gravitational field

The rough spherical particles characterized by interparticle friction coefficient ($\mu = 0.5$) and larger radius (R) were created randomly inside the larger box and allowed to settle down under the action of the gravity. A similar method was used to create lubricant particles characterized by smaller radius (r), $\mu = 0.05$ and were deposited on the top of the rough particles. This system is then sheared by moving one of the z-walls in the direction parallel to the x axis with constant velocity until the steady state is reached. Characterization of steady state is mentioned in section 2.3.3.

Negligible gravitational field

The rough ($\mu = 0.5$) and lubricant ($\mu = 0.05$) particles are both created randomly inside the larger box and then one of the z- wall was moved in z direction with constant velocity till the desired packing fraction is reached. Then, one of the z-wall was moved in positive x-direction with a) constant velocity and b) constant torque until the steady state is reached.

Friction reducing small (lubricant) particles

The small particle coat the surface of the rough, non-cohesive large particles, thereby reducing Coulombic friction between two large particles. The interparticle friction between small particles is quite small. While there is cohesion between a large and a small particle, there is no cohesive force between two large and two small particles.

Lubricant as cohesion reducing agent

In this case, the cohesion between two large particles is reduced by the presence of non-cohesive small particles in between. The distance dependant cohesive force is reduced due to increased distance between large particles. The interparticle friction between all the particles is kept constant. The cohesion between two small particles is negligible.

2.3.2 Particle Characteristics

The key parameters related to the particles are mentioned in the table 2.1. The values more or less correspond to those for glass (sodalime) beads, typically used to validate simulation results by experimental data [48].

parameter	value
Young's Modulus	$5 \times (10^7)$ pascals
Poisson's ratio	0.24
Coeff. of restitution	0.88
Coeff. of friction for rough particles	0.5
Coeff. of friction for lubricant	0.05
Coeff. of rolling friction	0.01
Density	2500 Kg/m^3
Timestep	0.000000125 sec
Mean diameter of the large particles	1 mm

Table 2.1: Properties of particles used in simulation.

The Young's modulus for both rough ($\mu = 0.5$) particles and lubricant ($\mu = 0.05$) is set to be equal to 5×10^7 Pascal. This value is less than the realistic values for Young's modulus (Y). The minimum value of the timestep required to compute the collision dynamics between two grains scales as $Y^{1/2}$ [48]. Higher realistic values of Young's modulus($O[10] \sim 12$) require very low value of time step which inturn increases the computation time. For the lower value of Young's modulus with proper values of timestep, the behaviour shown in the experiments was replicated by Silbert et. al. using DEM simulations [48]. Four values were considered for ratio of the size of large to small particles 1:5, 1:10, 1:15 and 1:20. Packing fraction ϕ_P for rough particles poured in presence of gravity is around 0.6. In the presence of the negligible gravity, shear induced segregation of the lubricant was observed for $\phi_p = 0.6$ [49]. To prevent this, presence uniform of shear was required in the system which was achieved at $\phi_p = 0.58$

The size ratio (s) is defined as ratio of the diameter of small, lubricant particle(d_l) and diameter of large grain(d).

$$s = \frac{d_l}{d}$$

The number ratio(n) is defined as ratio of the number of the lubricant particles(N_l) and

number of large grains(N_g)

$$n = \frac{N_l}{N_g}$$

The lubricant volume fraction (ϕ_{lg}) is defined as ratio of the total of the lubricant particles (V_l) to the total volume of the large grains(V_g).

$$\phi_{lg} = \frac{V_l}{V_g}$$
$$= ns^3$$

2.3.3 Velocity profile and steady state characterization

The instantaneous velocities of the grains were collected as output from the LIGGGHTS on the regular intervals during the period of the simulation. The shear cell was divided into 20 bins of the equal size $10d \times 10d \times 1d$. Each bin was assigned a velocity obtained by averaging the velocities of all the grains inside the bin at corresponding timestep. This gives the instantaneous velocity profile along the (shear) z-direction. The steady state is characterized by fluctuations of instantaneous velocity profile around the mean velocity profile ($10 \sim 12\%$). Finally, steady state profile was obtained by time averaging instantaneous velocity profiles. The steady state was achieved after 1.75 seconds of shearing.

Chapter 3

Lubrication by Friction Reduction

Previous studies show that the lubricant particles added to the blend are characterized by lesser frictional interaction [25]. These particles are cohesive in nature and coat the surface of the large particles thereby preventing the friction between them. The study of the flow of such system is presented over here.

3.1   Methodology

The detailed of methodology used to shear the system in absence as well as presence of lubricant particles are listed here.

3.1.1   Shear flow in absence of lubricant particles

The results for the blend without lubricant particle will act as reference against which all the subsequent results from simulation involving lubrication will be compared. Initially only rough ($\mu = 0.5$), non-cohesive mono-dispersed particles without lubricants were sheared in a $5d \times 10d \times 20d$ box by moving the rough planar wall, perpendicular to z axis in positive x direction with constant velocity. The gravity (9.8 m/s^2) was acting in negative y direction. The box is periodic in x direction. A planar rough wall is created at $y = 0$ to support grains. The moving planar wall doesn't impart significant shear on the system and simply slides

past the grains. To prevent this, the shearing wall was constructed of 2D planar square array of the spherical particles of same size and same elastic and frictional properties as particles being sheared. This modification increased the effective roughness of the wall and resulted in shearing of the particles inside. At higher shear velocities, particles near the wall crystallized, resulting in the motionless configuration due to over crowding also called jamming of the system. To encounter this problem poly-dispersity (10% with gaussian distribution) was introduced in the size of the rough particles. Using these polydispersed particles an exponential velocity profile was obtained for two different coefficient of friction (see fig. 3.2). The velocities are measured for the particles between $y = 4d$ and $y = 7d$ and averaging over the bins of size $1d \times 1d \times 1d$ in x and y direction. The qualitative nature of the profile remains the same over the range of velocities (10 - 1000 diameter/s). Given that the interparticle coefficient of friction between lubricant particles is maintained at 0.05, the large sized particles with reduced friction coefficient ($\mu = 0.05$) would represent the scenario of complete coating of rough ($\mu = 0.5$) with smaller lubricant particles, thereby providing the highest degree of lubrication.
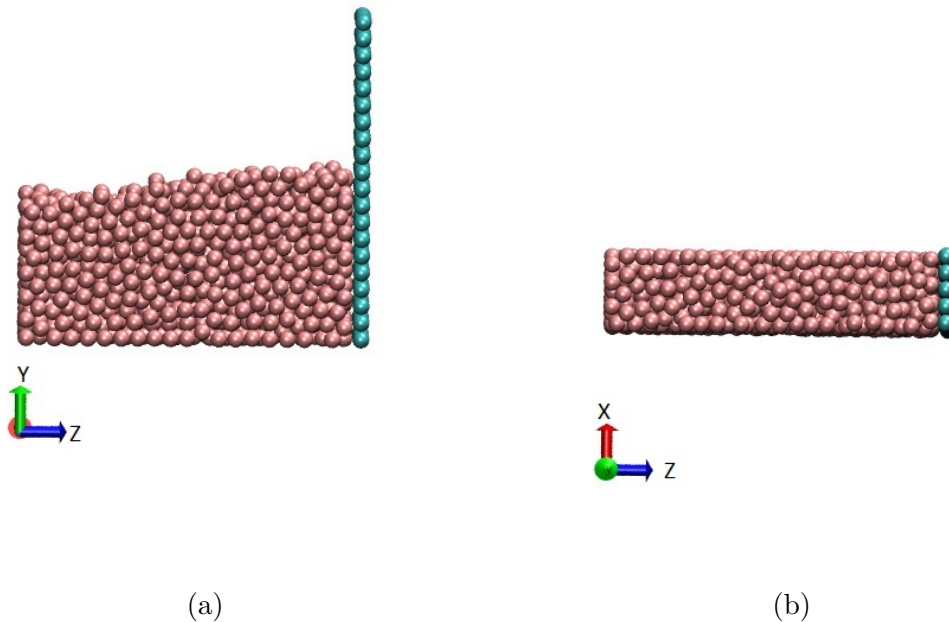

(a)   (b)

Figure 3.1: Schematic of the simulation in the shearcell a) cross section in y-z plane b) cross section in x-z plane
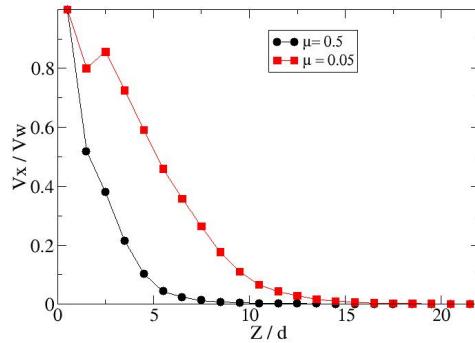
Figure 3.2: Time averaged and normalized velocity profile for two different interparticle coefficient of friction. velocities are normalized with the wall velocity. Profile has exponential nature with the higher velocities for lower value of coefficient of friction

3.1.2 Shear flow in presence of lubricant particles

In the following, we discuss the qualitative behavior of the system being sheared in presence of lubricant particles for various shear scenarios.

Shear by moving one boundary

The blend of small and large particles was sheared in the box with dimension $10d \times 10d \times 20d$ with wall velocity 5 diameter/s for a range of cohesion strengths (10^5 to 10^6 J/m^3). The width in x-dimension was increased for better understanding of spatial distribution of lubricant. The number ratio of large particles to small particles (n) is kept 10:1, while size ratio of large particles to small particles (s) is kept 5:1. For low cohesion strength, the lubricant particles percolated downward through sheared region near the moving wall and improvement in the instantaneous velocity profile in that region was observed. However over a longer time period the lubricant particles separated from the larger sized rough particles (see fig. 3.3). To prevent this segregation, higher cohesion strengths were used in subsequent simulations but that led to reduced flowability of the mixture and beyond a certain value lubricant was not able to percolate down and mixture was clogged. The presence of such a localized flow profile resulted in non-uniform mixing of lubricant particles, thereby creating two different behaviours. To prevent this scenario, shearing was carried out with both walls

27

moving at same speed but in opposite direction to each other as described next (see fig. 3.5).

(a)   (b)
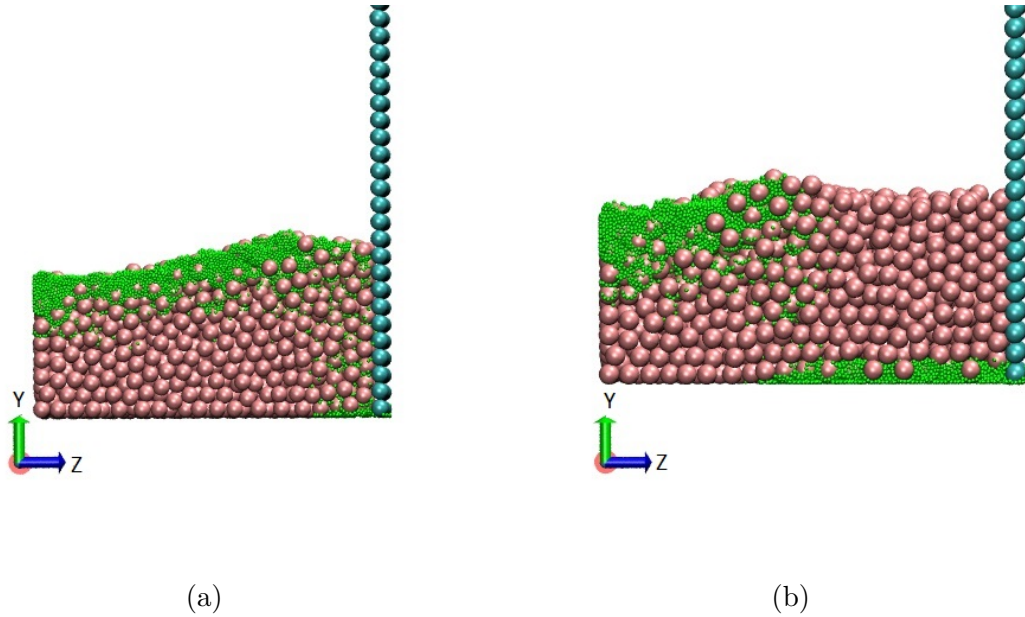
Figure 3.3: Shearing of the particles with lubricants a)lubricant particles percolating through the mixture b) Segregation of the lubricant in the moving area

Shear by moving both boundaries

Figure 3.2 indicates that the shear penetration depth for parallel plate shear is around 5-6 particle diameters. Hence to eliminate the non-moving part of the system, the shear thickness was reduced to 10 particle diameters and both walls were moved in opposite direction. This resulted in a significant portion of the system in a sheared state with a small region at the center remaining nearly stationary. The shear gradient, however, remains exponential through out (see fig. 3.4). Given the larger mobile region compared to that with single wall shearing, the chances for the mixing of the lubricant particles was expected to be high and thereby allowing to explore higher cohesion strengths.
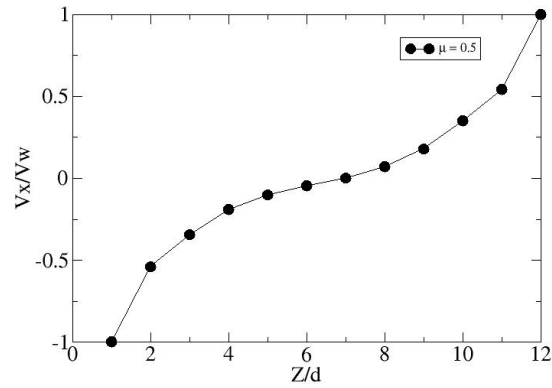
Figure 3.4: Velocity profile with small region at center with low velocities when sheared with both walls (z=0) and (z=12) moving in opposite direction with equal speed. Particle velocities are normalized by wall velocities.
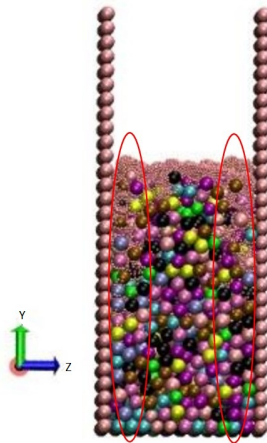
Figure 3.5: Cross section of the shearcell in Y-Z plane with both walls moving in opposite direction. Red ellipses shows moving areas and the central part inbetween is clogged.

The problem of non-uniform mixing and clogging at higher cohesion strengths, however persisted in this scenario as well. We also tried pouring lubricant at regular interval in

the moving mixture to avoid the clogging due to excess concentration of lubricant near the free surface but clogging persisted as the desired concentration of lubricant is reached. The clogging was mainly observed in the central area away from moving wall while motion was observed in areas near moving walls. The primary reason for this being the non-uniform shear rate in the system which leads to different levels of mixing, segregation and clogging in different regions. A linear profile with constant shear rate in the system is desirable to achieve uniform mixing through out the system which is possible in the absence of the gravity which is discussed next.

3.1.3   Shear Flow in negligible gravity

Simulations were carried out in the presence of the negligible gravitational force ($g = 10^{-6}m/s^2$) for the same particle characteristics. The behavior without the presence of lubricants is studied first followed by qualitative difference in the behavior due to presence of the lubricant.

3.1.4   Shear without lubricants

Polydispersed particles were sheared in shear cell of dimension $10d \times 10d \times 20d$ with the wall at z=20d moving at velocity $100d/s$. The wall particle diameter was kept twice that of sheared particles for better roughness (see fig. 3.6). This resulted in near linear velocity profile throughout as shown in fig. 3.7. The linear profile is achieved because of the lesser magnitude of contact forces than that present in the presence of gravity where the grains have to support the weight of the grains above them. Lesser amount of contact forces reduces the dissipation in the system.

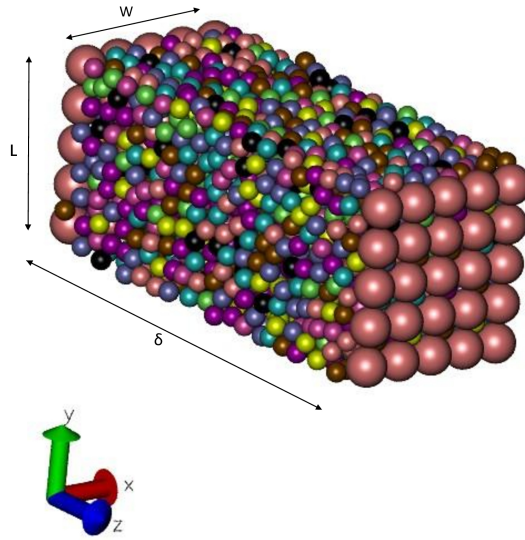Figure 3.6: Shear cell for simulation in presence of negligible gravity with the dimension $10d \times 10d \times 20d$ with periodic boundary condition in x and y-direction. Wall particles have size doubled to that of sheared particles.
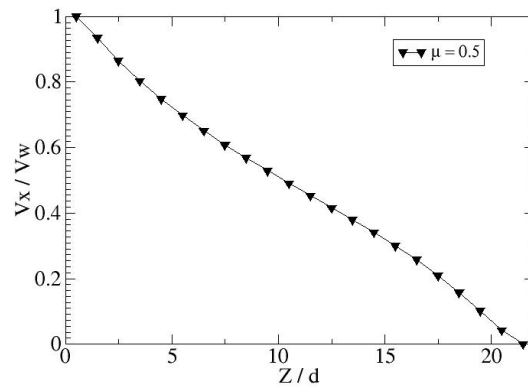
Figure 3.7: Velocity profile for $\mu = 0.5$ in the parallel plate shear geometry in the presence of negligible gravity. Velocities are normalized with the wall velocity

Linear profile with velocities fixed at the both end ($100d/s$ at one wall and $0d/s$ at opposite wall) will have very little room for improvement when lubricated. To see more pronounced effect of lubrication in the system, we shear the system by applying constant torque on wall instead of moving it with constant velocity. Constant force of 10^{-5} N directed in x-axis was applied to each particle on the wall. All the subsequent simulations are involve constant torque of same magnitude and direction.
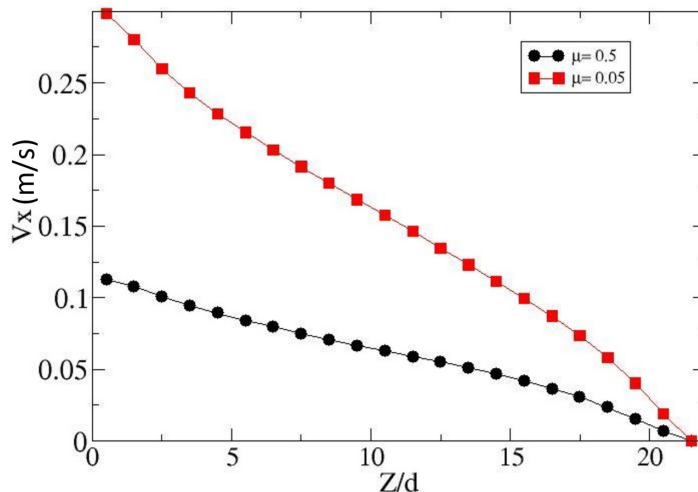
Figure 3.8: Velocity Profile for two coefficient of frictions in negligible gravity when sheared by applying constant torque. The wall at (z=20d) was sheared by applying constant force of 10^-5 N on each wall particle.

Shearing by constant torque allows variable moving wall velocities. Steady state is characterized by fluctuation in a profile about some mean and different parameters would generate profiles with different wall velocities in the steady state. Reduced coefficient of friction resulted in higher wall velocity which is expected due to reduced interparticle frictional forces (see fig. 3.8).

3.1.5   Shear with lubricants

The bidispersed mixture consisting of large, rough particles and small, lubricant particles was sheared in the shearcell of the same dimension as mentioned in section 3.2.1 by applying constant torque of 10^{-5} N. The large to small particle size ratio is kept at 5:1. The cohesion

strength between large and small particle is kept at 50000 J/m^3. Simulation were carried for three different number ratios (n) of small and large viz 2.5:1, 5:1 and 10:1. The velocity profiles are shown in the fig 3.9.

3.2   Results and discussion

Increasing the concentration of the lubricant particles shows monotonic decrease in velocity magnitude. Thus inclusion of the lubricant is having adverse effect on the flow properties, the probable cause being the large size of the lubricant particles used. Larger the size of the lubricant particle, smaller is the probability for it to be in between two large particles. For lubrication by reducing the friction, we need at least two lubricant particles in between large particles which has even less probability (fig. 3.10). Increasing the number of the lubricant particles might increase the probability but this results lower velocity profile due to increased volume fraction as shown in fig. 3.9. The alternative is to reduce the particle size to accommodate mare number of particles leading to increased probability of lubricant particles leading to increased probability of lubricant particles between large particles.
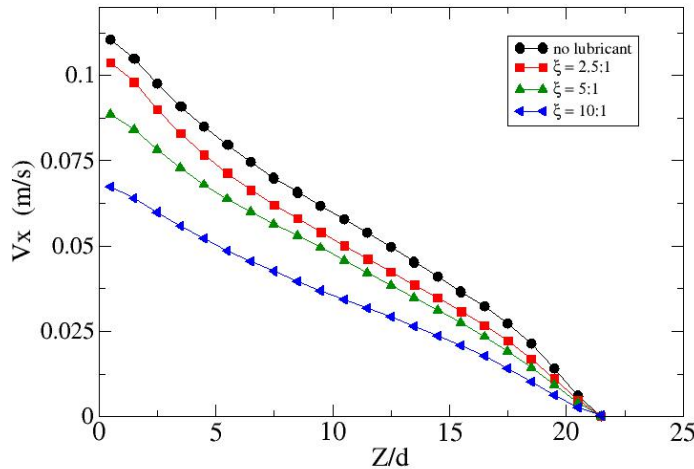
Figure 3.9: Velocity profiles with varying n when sheared in presence of lubricant by applying constant torque in negligible gravity

<div align="center">(a)   (b)</div>
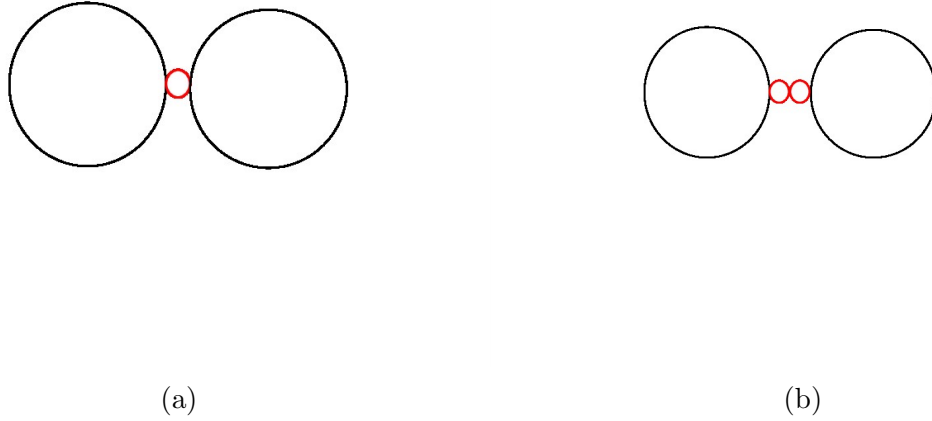
Figure 3.10: Representation of two different configurations of small and large particles. Small red particles are lubricants and large black particles are rough a)one lubricant particle inbetween b)two lubricant particles inbetween

3.3 Concluding Remarks

Magnesium stearate, which is the most used lubricant, has plate-like structure which results in higher surface to volume ratio which helps to coat the rough particle efficiently. This can only be mimicked by smaller sized spherical lubricant particles which provide higher surface to volume ratio. The probability that lubricant particle will come in space between rough particle also increases with the reduction in the size and small lubricant particles also occupy smaller volume fraction than large lubricant particles for the same number of particles resulting in less crowding behavior. Hence, with smaller size of the lubricant probability of lubrication increases. The simulations with the reduced lubricant particle size are currently under progress.

Chapter 4

Lubrication by Cohesion Reduction

The grains of the pharmaceutical blends are cohesive in nature. Due to this cohesive force, the blend particles stick to each other as well as with the walls. This reduces the overall flow rate. As mentioned in section 2.3.1, lubricant helps to reduce this cohesive force by increasing the distance between cohesive particles. The increased distance tends to break the contact between two particles which results in nearly zero cohesive force. The lubricant particles are required to be non-cohesive in nature. The study of the flow of such system is detailed over here.

4.1 Methodology

The system was prepared as mentioned in the section 2.3.1. Polydispersed, cohesive particles were sheared in the shearcell of the dimension $10d \times 10d \times 20d$ by applying constant torque (10^{-5}) in x-direction in presence of negligible gravity (same as mentioned in sec.3.1.3)(fig. 4.1). Wall particle diameter is also kept twice that of sheared particles to increase th effective roughness of the wall. The cohesion strength k between two large particles is 5×10^4 J/m^3. The size ratio (s), number ratio (n) and lubricant volume fraction (ϕ_{lg}) are the same as defined in the section 2.3.2. The steady state velocity profiles were calculated in similar manner as mentioned in section 2.3.3. A near linear velocity profile was observed for this case (see fig. 4.2).
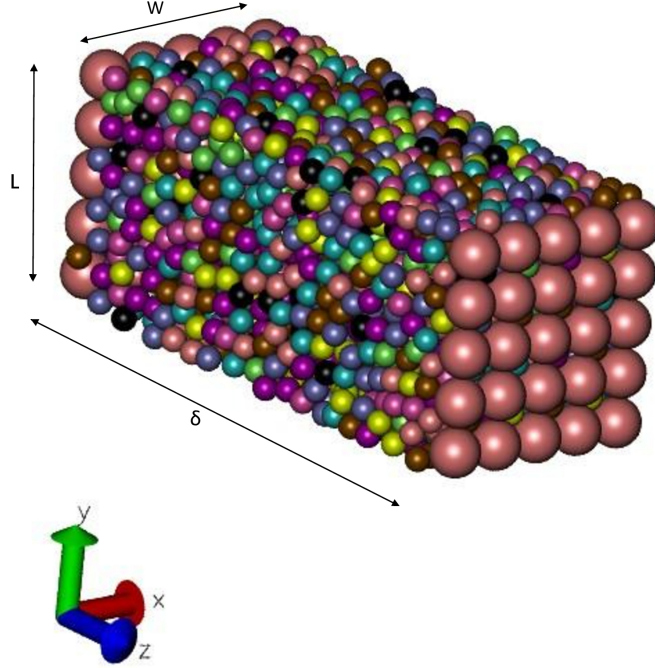
Figure 4.1: Shear cell for simulation in presence of negligible gravity with the dimension $10d \times 10d \times 20d$ with periodic boundary condition in x and y-direction. Wall particles have size doubled to that of sheared particles.

Bidispersed mixture consisting of large, rough, cohesive particles and small, non-cohesive lubricant particles was sheared in the same shearcell by applying constant torque (10^{-5}) on wall at $Z = 20$ d. The small and large lubricant size ratio is maintained constant at 20:1. The simulation were carried out for different number ratios(n). The values of n were varied from 50:1 to 150:1 with constant increment of 25. For this variation, lubricant volume fraction (ϕ_{lg}) changes with 0.003125 with each increment. The steady state velocity profiles were calculated as mentioned in the section 2.3.3. In the next section we describe the effect of varying lubricant size ratio (s) to qualitatively obtain the dependence of the lubrication on the lubricant size. The value of s was varied from 0.05 to 0.2 with constant lubricant volume
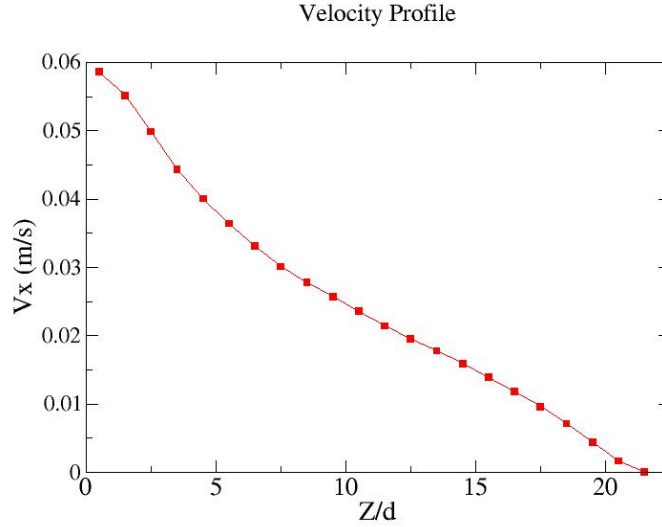
Figure 4.2: Velocity profile for the cohesive particles sheared in the shearcell by applying the constant torque on the wall in x-direction(10^{-5} N).

fraction.

4.2 Results and Discussion

The detailed discussion about effect on lubrication by varying number ratio(n) and size ratio(s) is discussed in this section.

4.2.1 Varying lubricant concentration

The velocity profiles in absence and presence of lubricant for different number ratios are shown in fig. 4.3. The lubricant effect is primarily seen in the region of high shear ($z/d < 10$) beyond which the profiles are nearly the same. The higher shear region represent the rapid movement for rough as well as lubricant particles for given run time of the simulation. This ensures higher number of contact breaking and their re-creation with lubricant particles compared to lower shear region ($z/d > 10$) which allows higher degree of lubrication.
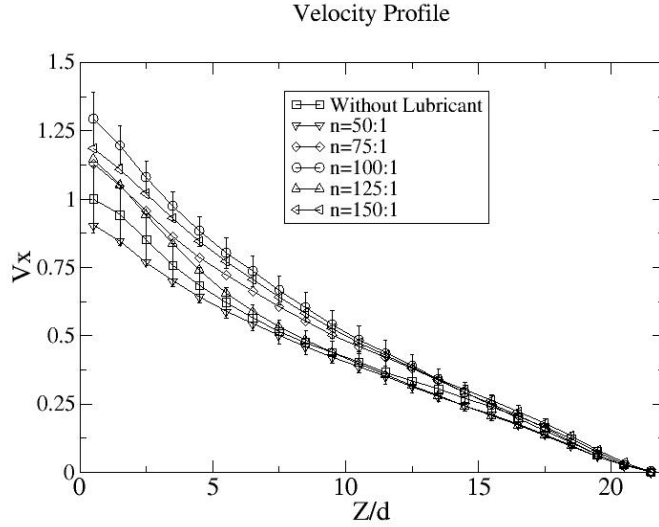
Figure 4.3: Velocity profiles when sheared by applying constant torque(10^{-5} N) with varying number ratio n_r from 0 (no lubricant) to 150:1 . All the velocities are normalized with the wall velocity in the absence of lubricant.

For region $(z/d < 10)$, the velocity magnitude first increases with increasing n followed by decrease at higher n with maximum at $n = 100$:1. As we increase the concentration of the lubricant, more number of lubricant particles surround the cohesive large particle thereby increasing the probability of lubrication with higher n. The exact effect of lubrication is however not clear given different variation of velocities in different region.

To quantify the effect of lubrication, we calculate a quantity granular flux f_g. Granular flux is defined as volumetric flux of the grains in the flow direction across the x-plane of the shear cell, effectively the flow rate and is obtained from area enclosed by each velocity profile.

$$f_g = \int_{z=0}^{z=20d} \vec{v}.d\vec{A} = \int_{z=0}^{z=20d} v_x dA = \Delta y \int_{z=0}^{z=20d} v_x dz$$

Where $\Delta y = 10d$ is the width of the system in y-direction. To evaluate this integration, the trapeziodal method of integration was used with $\delta z = 1d$. Hence, the integration simplifies to

$$f_g \approx 10d \sum_{z=1}^{z=19} \frac{v_x(k) + v_x(k+1)}{2}$$

38

Fig. 4.4 shows the variation of the f_g with number ratio. The error-bars indicate the standard deviation in the flux values at steady state. The flux is equal to $4.61 \times 10^-6 m^3/s$ in absence of lubricant. When n is increased by 50 from zero slight decrease in the granular flux is observed. This suggests that insufficient concentration of lubricant, perhaps has an adverse effect on the flow. The probable reason behind such behavior is that the number of lubricant particles surrounding the cohesive particles are not enough to reduce the cohesive contacts and inherent dissipative nature of the collision of small particles with cohesive large particle causes further dissipation in the flow. With further increase in n, value of the f_g is observed to be higher than that for the case without lubricant, suggesting that lubrication occurs. With increasing n the, the number of the lubricant particles surrounding the cohesive particle increases as shown in fig 4.5, leading to higher probability of the lubrication. For further increase in n, the oscillates around a constant value of 5×10^-6 suggesting lubrication in all the cases. It is not clear whether the flux will decrease for much higher increase of n (possibly due to crowding) or whether it will remain the same. This work, to determine the precise state of over-lubrication, and its manifestation in terms of velocity profile is currently under progress.
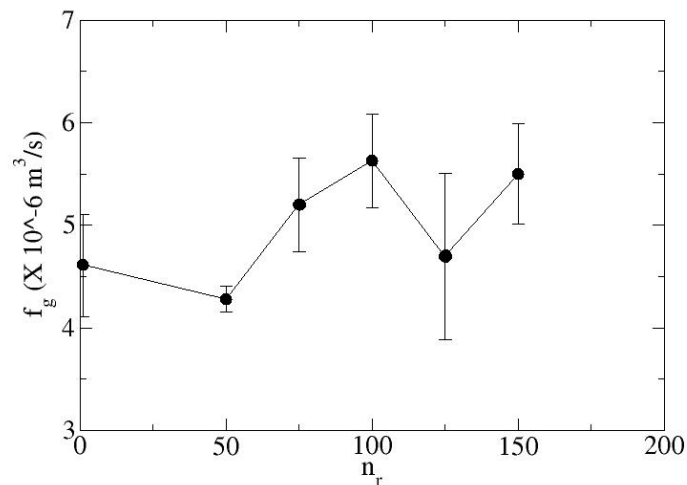
Figure 4.4: Granular flux as function of number ratio(n). Error bars indicate standard deviation in the flux value.
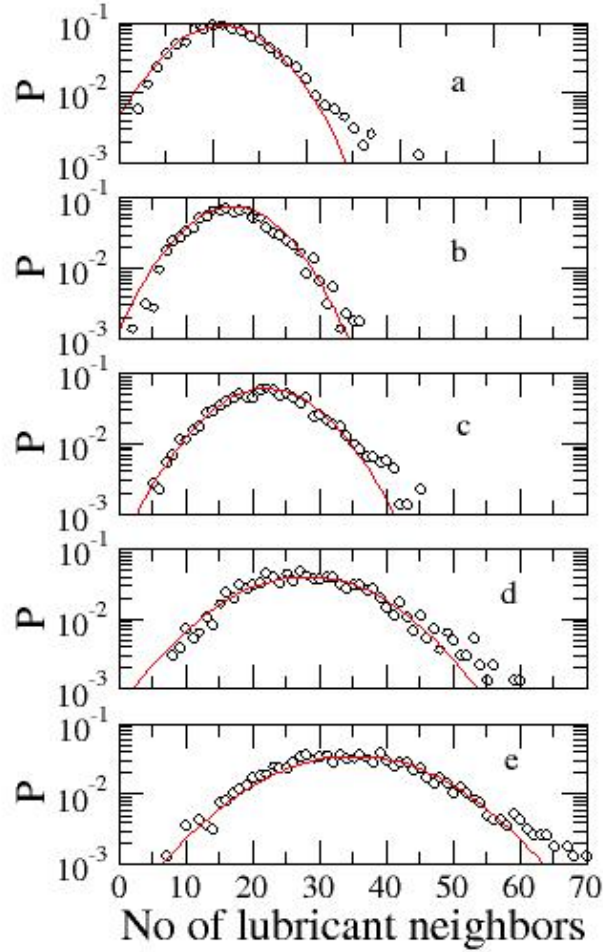
Figure 4.5: Probability (P) distribution of number of lubricant neighbors for cohesive particles for various n. The y-axis is in the logarithmic scale. The probability distribution closely follow Gaussian distribution and as n increases the distribution becomes more wide and mean value also increases.a) n=50:1 mean=11 variance=40 b) n=75:1 mean=17 variance=70 c) n=100:1 mean=22 variance=90 d) n=125:1 mean=28 variance=180 e) n=150:1 mean=35 variance=230

Further characterization of system shows that distribution of the lubricant is nearly uniform throughout the shear cell (not shown here). To further probe the spacial variation of lubricant particles, we calculate their distribution around every large particle. Though

lubricant is uniformly distributed in the system, the number of the lubricant neighbors(l) to cohesive particle is not the same for each cohesive particle and varies across the sample. Since there is no cohesive force between the large and small particles, it is very less probable that in given snapshot we will find sufficient number of lubricant particles touching with the large particle. We,thus, define a lubricant particle to be neighbor of the cohesive particle if distance between lubricant and cohesive particle is less than $\frac{d_g+2d_l}{2}$, where d_g and d_l are the diameter of the cohesive and lubricant particles respectively. The distribution of number of lubricant neighbors is shown in fig. 4.5. The number of lubricant neighbors are distributed normally with increasing mean and spread of the distribution with increasing n, thereby ensuring larger number of cohesive particle having a higher number of lubricant neighbors as n increases which results in higher granular flux due to higher lubrication.

4.2.2   Changing lubricant size ratio

The effect of size ratio on the lubrication behavior is investigated for fixed volume fraction ($\phi_l g$), hence changing s at constant ϕ_c. Figure 4.8 shows the velocity profiles for four different size ratios. The magnitude of velocity increases monotonically with increasing s. The effect is, however more pronounced for regions with higher velocity. The small effect is nearly expected for $z/d > 12$ given that the flow is nearly stationary in this region. The granular flux is calculated for the four values of s is shown in fig. 4.7. The error bars denote the standard deviation in fig 4.7.

As expected, the granular flux shows a monotonic increase with decrease in the value of s. The decrease in s is accompanied by an increase in n, to maintain constant volume of lubricant particles. This essentially increases the surface coverage of large particles by an increasingly large number of lubricant particles thereby decreasing the probability of two large particles coming in contact. Very low value of $s << 0.05$ will, then approximate the typical coverage by a plate like magnesium stearate lubricant. It is expected that the flux will asymptotically reach a constant value at a certain small value of s, the investigation of which are in progress. The red dashed line in the graph indicates the granular flux of the non-lubricated system. Only $s = 0.067$ and $s = 0.05$ have higher flux than that of non-lubricated system. This suggests that there exists a critical size of the lubricant above which lubrication will not be achievable.

41
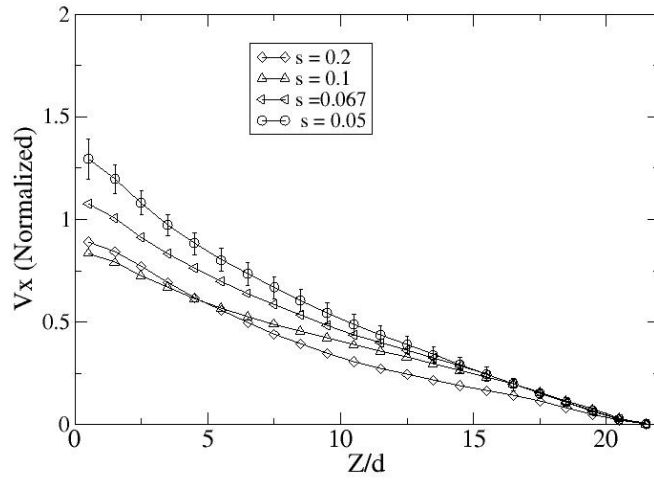
Figure 4.6: Velocity profiles when sheared by applying constant torque(10^{-5} N) with varying size ratio s from 0.05 to 0.2. All the velocities are normalized with the wall velocity in the absence of lubricant.
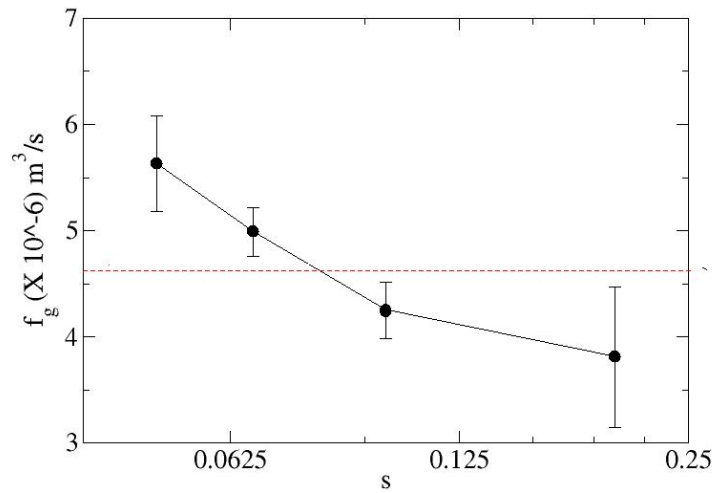
Figure 4.7: Granular flux as function of size ratio(s_r). Bars indicate standard deviation in the flux value. The red dashed line indicates $f_g = 4.61 \times 10^{-6} m^3/s$, the granular flux for non-lubricated system. Here x-axis is in logarithmic scale.

4.3   Concluding Remarks

The lubrication of granular flow by reducing the cohesive force between two large grain was studied in this chapter. The mixture containing the large, cohesive particles and small, cohesion less lubricant particles was sheared in parallel plate geometry for the range of concentration and size of lubricant particles. The granular flux increases with increasing concentration of lubricant and decreasing size of the lubricant. The lubrication was not achieved below critical value of lubricant concentration and above critical value of lubricant size. The extreme limits of increased concentration and decreased size of lubricant particles are currently under investigation which will give better insights into lubrication behavior.

Chapter 5

Conclusion and Future outlook

The flow of pharmaceutical powders are governed by frictional and cohesive interaction of constituent particles. To modify the flow behavior, a small amount of lubricant powder is added. This lubricant powder coats the surface of the rough particles resulting in reduced friction and/or cohesion between two rough particle,thereby improving the flow. We use DEM simulations to study shear flow of the lubricated mixture of the grains. The blend particles are modeled as large sized, rough ($\mu = 0.5$), spherical particles and lubricant particles are modeled as small sized, spherical particles with lesser frictional interactions ($\mu = 0.05$). We study two mechanism of lubrication viz, lubrication by reducing friction between large particles and lubrication by reducing cohesion between large particles in the parallel plate shear geometry. The shear flow was studied in the presence as well as absence of gravitational field. We varied the concentration and size of the lubricant particles to study its effect qualitatively on the degree of the lubrication.

The modified shear behavior was quantified in terms of granular flux for a constant applied torque to the system. The behavior of this flux was studied for two cases viz. presence of lubricant particles to reduce friction and to reduce cohesion. In the latter case, for the ranges of particle number ratio and size ratio studied, the flux shows an increase with increase in number ratio and decrease in size ratio. Both variation seem to increase the number of lubricant particles between large particles, thereby preventing the contact between them, hence reducing the cohesive force resulting in improved flow. The extreme limits of increased n and decreased s are currently under investigation which may lead to

overlubrication. The lubrication was seen to be absent above a critical value of s and below critical value of n. The study regarding the reduction of friction between large particles due to lubricant particles is currently under progress.

The overall work gives a qualitative insights into the process of lubrication of powder flow using a small sized powders. The results offer a glimpse into the rich behavior that this systems provides which should pave the way for better theoretical understanding. Comparison of results with experiments, being performed in the lab, will provide better characterization of simulation parameters. However, further work is necessary to obtain detailed quantification of the lubricant phenomenon and also about the detailed mechanism of lubrication. More importantly, simulations using aspherical lubricant particles will provide insights more closer to the actual pharmaceutical process.

Bibliography

[1] P. G. de Gennes. Granular matter: a tentative view. *Rev. Mod. Phys.*, 71:S374–S382, Mar 1999.

[2] Changquan Calvin Sun. Decoding powder tabletability: Roles of particle adhesion and plasticity. *Journal of Adhesion Science and Technology*, 25(4-5):483–499, 2011.

[3] Lakio Satu, Vajna Bal, Istv Farkas, and Henri Salokangas. Challenges in detecting magnesium stearate distribution in tablets. *AAPS PharmSciTech*, 2013.

[4] Fernando J Muzzio, Troy Shinbrot, and Benjamin J Glasser. Powder technology in the pharmaceutical industry: the need to catch up fast. *Powder Technology*, 124(1):1 – 7, 2002.

[5] Joseph Kushner and Francis Moore. Scale-up model describing the impact of lubrication on tablet tensile strength. *International Journal of Pharmaceutics*, 399(1):19 – 30, 2010.

[6] R. M. Nedderman. *Statics and Kinematics of Granular Materials*. Cambridge University Press, 1992.

[7] C S Campbell. Rapid granular flows. *Annual Review of Fluid Mechanics*, 22(1):57–90, 1990.

[8] I. Goldhirsch. Scales and kinetics of granular flows. *Chaos: An Interdisciplinary Journal of Nonlinear Science*, 9(3):659–672, 1999.

[9] Olivier Pouliquen and Franois Chevoir. Dense flows of dry granular material. *Comptes Rendus Physique*, 3(2):163 – 175, 2002.

[10] GDR MiDi. On dense granular flows. *The European Physical Journal E*, 14(4):341–365, Aug 2004.

[11] Saloome Siavoshi, Ashish V. Orpe, and Arshad Kudrolli. Friction of a slider on a granular layer: Nonmonotonic thickness dependence and effect of boundary conditions. *Phys. Rev. E*, 73:010301, Jan 2006.

[12] J.-C. Tsai, G. A. Voth, and J. P. Gollub. Internal granular dynamics, shear-induced crystallization, and compaction steps. *Phys. Rev. Lett.*, 91:064301, Aug 2003.

[13] V. V. R. Natarajan, M. L. Hunt, and E. D. Taylor. Local measurements of velocity fluctuations and diffusion coefficients for a granular material flow. *Journal of Fluid Mechanics*, 304:125, 1995.

[14] O. Pouliquen. Scaling laws in granular flows down rough inclined planes. *Physics of Fluids*, 11(3):542–548, 1999.

[15] Ashish V. Orpe and D. V. Khakhar. Solid-fluid transition in a granular shear flow. *Phys. Rev. Lett.*, 93:068001, Aug 2004.

[16] D. V. KHAKHAR, ASHISH V. ORPE, PETER ANDRESN, and J. M. OTTINO. Surface flow of granular materials: model and experiments in heap formation. *Journal of Fluid Mechanics*, 441:255264, 2001.

[17] A review of dry particulate lubrication: Powder and granular materials. *Journal of Tribology*, 129:438 – 449, 2007.

[18] Granular flow lubrication: Continuum modeling of shear behavior. *Jounal of Tribology*, 3:499–510, 2004.

[19] Maurice Godet. The third-body approach: A mechanical view of wear. *Wear*, 100(1):437 – 452, 1984.

[20] Brendle M. Berthier Y, Godet M. Velocity accommodation in friction. *Tribology Transections*, 32:490–496, 1989.

[21] Berthier Y. Experimental evidence for friction and wear modeling. *Wear*, 32:490–496, 1989.

[22] S. Descartes, C. Desrayaud, E. Niccolini, and Y. Berthier. Presence and role of the third body in a wheelrail contact. *Wear*, 258(7):1081 – 1090, 2005. Contact Mechanics and Wear of Rail/Wheel Systems.

[23] Iordanoff II, Seve BB, and Berthier YY. Simulation of wear through mass balance in dry contact. *ASME J. Tribol.*, 124:530–538, 2002.

[24] Fillot N, Iordano I, and Berthier Y. Solid third body analysis using a discrete approach: Influence of adhesion and particle size on macroscopic properties. *ASME J. Tribol.*, 127, 1984.

[25] Yifan Wang, Juan G. Osorio, Tianyi Li, and Fernando J. Muzzio. Controlled shear system and resonant acoustic mixing: Effects on lubrication and flow properties of pharmaceutical blends. *Powder Technology*, 322:332 – 339, 2017.

[26] Qi (Tony) Zhou, John A. Denman, Thomas Gengenbach, Shyamal Das, Li Qu, Hailong Zhang, Ian Larson, Peter J. Stewart, and David A.V. Morton. Characterization of the surface properties of a model pharmaceutical fine powder modified with a pharmaceutical lubricant to improve flow via a mechanical dry coating approach. *Journal of Pharmaceutical Sciences*, 100(8):3421 – 3430, 2011.

[27] S Jonat, S Hasenzahl, M Drechsler, P Albers, K.G Wagner, and P.C Schmidt. Investigation of compacted hydrophilic and hydrophobic colloidal silicon dioxides as glidants for pharmaceutical excipients. *Powder Technology*, 141(1):31 – 43, 2004.

[28] Ingfried Zimmermann, M. Eber, and K. Meyer. Nanomaterials as flow regulators in dry powders. *International journal of research in physical chemistry and chemical physics*, 2009.

[29] Jinjiang Li and Yongmei Wu. Lubricants in pharmaceutical solid dosage forms. *Lubricants*, 2014.

[30] Rafael Mendez, Fernando J. Muzzio, and Carlos Velazquez. Powder hydrophobicity and flow properties: Effect of feed frame design and operating parameters. *AIChE Journal*, 58(3):697–706, 2012.

[31] Pintye-Hdi K, Tth I, and Kata M. Investigation of the formation of magnesium stearate film by energy dispersive x-ray microanalysis. *Pharm Acta Helv*, 1981.

[32] Davies MC, Brown A, and Newton JM. Chemical characterization of lubricant films. *J Pharm Pharmacol*, 1987.

[33] M Celik. Compaction of multiparticulate oral dosage forms, multiparticulate oral drug delivery. *Drugs and Pharmaceutical Sciences*, 1994.

[34] Jennifer Wang, Hong Wen, and Divyakant Desai. Lubrication in tablet formulations. *European Journal of Pharmaceutics and Biopharmaceutics*, 75(1):1 – 15, 2010.

[35] Joseph Kushner and Francis Moore. Scale-up model describing the impact of lubrication on tablet tensile strength. *International Journal of Pharmaceutics*, 399(1):19 – 30, 2010.

[36] Amit Mehrotra, Marcos Llusa, Abdul Faqih, Michael Levin, and Fernando J. Muzzio. Influence of shear intensity and total shear on properties of blends and tablets of lactose and cellulose lubricated with magnesium stearate. *International Journal of Pharmaceutics*, 336(2):284 – 291, 2007.

[37] Peter A Cundall and Otto DL Strack. A discrete numerical model for granular assemblies. *Geotechnique*, 1979.

[38] J. M. Haile, Ian Johnston, A. John Mallinckrodt, and Susan McKay. Molecular dynamics simulation: Elementary methods. *Computers in Physics*, 7(6):625–625, 1993.

[39] Loup Verlet. Computer "experiments" on classical fluids. i. thermodynamical properties of lennard-jones molecules. *Phys. Rev.*, 159:98–103, Jul 1967.

[40] William C. Swope, Hans C. Andersen, Peter H. Berens, and Kent R. Wilson. A computer simulation method for the calculation of equilibrium constants for the formation of physical clusters of molecules: Application to small water clusters. *The Journal of Chemical Physics*, 76(1):637–649, 1982.

[41] Lammps. http://lammps.sandia.gov.

[42] Steve Plimpton. Fast parallel algorithms for short-range molecular dynamics. *Journal of Computational Physics*, 117(1):1 – 19, 1995.

[43] Christoph Kloss, Christoph Goniva, Alice Hager, Stefan Amberger, and Stefan Pirker. Models, algorithms and validation for opensource dem and cfd-dem. *Progress in Computational Fluid Dynamics*, 12:140 – 152, 06 2012.

[44] Liggghts. https://www.cfdem.com.

[45] Alberto Di Renzo and Francesco Paolo Di Maio. Comparison of contact-force models for the simulation of collisions in dem-based granular flow codes. *Chemical Engineering Science*, 59(3):525 – 541, 2004.

[46] Kenneth Langstreth Johnson, Kevin Kendall, A. D. Roberts, and David Tabor. Surface energy and the contact of elastic solids. *The Royal Society*, 1971.

[47] W. F. Kern and J. R Bland. Solid mensuration with proofs, 2nd ed. *New York: Wiley,*, 1948.

[48] Leonardo E. Silbert, Deniz Ertaş, Gary S. Grest, Thomas C. Halsey, Dov Levine, and Steven J. Plimpton. Granular flow down an inclined plane: Bagnold scaling and rheology. *Phys. Rev. E*, 64:051302, Oct 2001.

[49] Katalin A. Gillemot, Ellk Somfai, and Tams Brzsnyi. Shear-driven segregation of dry granular materials with different friction coefficients. *Soft Matter*, 13:415–420, 2017.

[50] E.C. Abdullah and D. Geldart. The use of bulk density measurements as flowability indicators. *Powder Technology*, 102(2):151 – 165, 1999.

[51] *Flow properties of bulk solids*, pages 35–74. Springer Berlin Heidelberg, Berlin, Heidelberg, 2008.